CrystEngComm

Accepted Manuscript

This article can be cited before page numbers have been issued, to do this please use: G.ATTILIO ARDIZZOIA, S. Brenna, F. Civati, V. Colombo and A. Sironi, *CrystEngComm*, 2017, DOI: 10.1039/C7CE01404J.




ROYAL SOCIETY OF CHEMISTRY

rsc.li/crystengcomm

View Article Online
DOI: 10.1039/C7CE01404J

CrystEngComm

ARTICLE

# A Phosphorescent Copper(I) Coordination Polymer with Sodium 3,5-dimethyl-4-sulfonate pyrazolate

Received 00th January 20xx,
Accepted 00th January 20xx

DOI: 10.1039/x0xx00000x

www.rsc.org/

G. Attilio Ardizzoia,[a] Stefano Brenna,[a*] Francesco Civati,[b] Valentina Colombo[c*] and Angelo Sironi[c]

A phosphorescent copper(I) coordination polymer with the sodium salt of 3,5-dimethyl-4-sulfonate pyrazole (**$HL_{Na}$**) has been prepared and structurally characterized. The presence of the $SO_3Na$ substituent in position 4 of the pyrazole ring led to a 3D polymeric species in which an organic/inorganic/organic sandwich motif is observed and repeated along the *a* axis through zig-zag chains of linear coordinated Cu(I) ions. The inorganic core of the sandwich consists of a trapezoidal grid of Na-ions interconnected by μ-(κO;κ$^2$-O′,O″)-bridging sulfonates and bridging water molecules; H-bonds can be also found between water molecules and $SO_3^-$ groups. In the solid state, the copper derivative showed an interesting phosphorescent behavior when irradiated with UV light, with a yellow emission (570 nm) and a good absolute quantum yield ($\Phi_{PL}$ = 0.44), together with a remarkable Stokes shift of 2.50 eV.

## Introduction

Coinage metal(I) pyrazolate complexes exist in various arrangements, from infinite chain or planar trinuclear disposition, to the less common saddle-shaped tetranuclear and hexanuclear units.[1] Typically, the nuclearity of the parent pyrazole ligand is replicated in the corresponding M(I) pyrazolate compound,[2] where the metal replaces the former indolic hydrogen. Thus, [Cu(pz)][3] and [Ag(pz)][2,4] (Hpz = pyrazole) are described as infinite polymeric chains, [M(3,5-$R_2$-pz)]$_3$ (M = Cu, Ag, Au; R = Me, $^i$Pr, $CF_3$)[5] consist of trinuclear species with a $Cu_3N_6$ core, whereas large substituents (Ph, $^t$Bu, COO$^{sec}$Bu)[6] in the 3 and 5-positions of the pyrazolate ring lead to tetranuclear structures. In the case of 3,5-dimethyl pyrazolate derivatives the trinuclear structure is maintained even with very bulky groups like naphthyl or anthryl[7] at the 4-position.

In the past, we widely explored the coordination chemistry of N-based multidentate ligands,[8] with special attention to pyrazole and its analogues (imidazole, triazole) both in their neutral[9] and anionic azolate forms.[10] The corresponding metal complexes have found applications in catalysis,[8a-c] material science[9] or in the synthesis of oligonuclear systems.[6b] Among these investigations on N-based ligands, some of us recently conducted a study on the photophysical properties of zinc(II) and silver(I) compounds bearing 3-aryl-substituted 1-pyridylimidazo[1,5-*a*]pyridines.[11] Continuing the investigation on luminescent $d^{10}$-metal compounds with N-based ligands, herein we describe the synthesis of a phosphorescent copper(I) coordination polymer with the sodium salt of 3,5-dimethyl-4-sulfonate pyrazole (3,5-dimethyl-4-$SO_3$Na-1*H*-pyrazole, **$HL_{Na}$**). In particular, the stable species **$CuL_{Na}$** ([Cu(3,5-dimethyl-4-$SO_3$Na pyrazolate)], **1**) has been characterized by *ab-initio* structural solution methods on X-ray Powder Diffraction (XRPD) data, which revealed that in our system the metal centers are disposed in zig-zag chains, held together by the 3D motif imposed by the -$SO_3$Na substituent and water molecules in the lattice. In the solid state, compound **1** shows a notable phosphorescent behaviour when irradiated with UV light, with a yellow $\lambda_{max}$ of emission (570 nm), a good absolute quantum yield ($\Phi_{PL}$ = 0.44) and a very high Stokes shift (2.50 eV).

## Results and discussion

### Syntheses and characterization

The sodium salt of 3,5-dimethyl-4-sulfonate pyrazole (**$HL_{Na}$**) was prepared following the procedure reported by Ackerman[12] (Scheme 1a). First, 3,5-dimethyl-1*H*-pyrazole (3,5-Hdmpz) was sulfonated at position 4 with oleum; then, careful neutralization with $BaCO_3$ quantitatively allowed to isolate the corresponding barium salt (**$HL_{Ba}$**). Finally, a cation exchange with $Na_2SO_4$ in water afforded species **$HL_{Na}$** as a white, crystalline powder. Small crystallites, suitable for a XRD single-crystal diffraction experiment, were isolated from this powder (*vide infra*).

[a] *Dipartimento di Scienza e Alta Tecnologia, Università degli Studi dell'Insubria, Via Valleggio, 9, 22100 Como, Italy. E-mail: stefano.brenna@uninsubria.it*
[b] *School of Chemistry, National University of Ireland, University Road – H91 TK33 Galway, Ireland*
[c] *Department of Chemistry, University of Milan, via Golgi 19 – 20133 Milano, Italy. E-mail: valentina.colombo@unimi.it*

Electronic Supplementary Information (ESI) available: Infrared spectra of **$HL_{Na}$** and **1**; TGA/DSC spectra for **1**; fitting of the lifetime decay of complex **1**; further crystallographic information for **$HL_{Na}$** and **$CuL_{Na}$**. See DOI: 10.1039/x0xx00000x

View Article Online
DOI: 10.1039/C7CE01404J




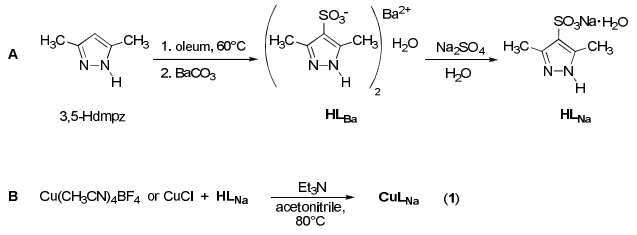


**Scheme 1**. (**A**) Synthesis of ligand $\mathbf{HL_{Na}}$ and (**B**) synthesis of complex $\mathbf{CuL_{Na}}$ (**1**).

The infrared spectrum of $\mathbf{HL_{Na}}$ (Figure S1) is characterized by a broad band at about 1200 $cm^{-1}$ due to the $SO_3$ group, together with two intense absorptions related to $\nu_{NH}$ stretching (3170 and 3110 $cm^{-1}$). The presence of one water molecule in the formula is confirmed by bands at 3518 and 3421 $cm^{-1}$ (stretching) and 1644 $cm^{-1}$ (bending). The $\nu_{CH}$ of methyl groups are noticed in the region 2970-2870 $cm^{-1}$ (Figure S2).

Complex $\mathbf{CuL_{Na}}$ (**1**) was isolated in good yields by gently refluxing a suspension of $Cu(CH_3CN)_4BF_4$ or CuCl with one equivalent of $\mathbf{HL_{Na}}$, in acetonitrile, in the presence of $Et_3N$ (Scheme 1B). $\mathbf{CuL_{Na}}$ was completely insoluble in organic solvents, thus preventing any attempt to obtain single crystals suitable for single crystal X-ray analysis (*vide infra*). Yet, **1** was obtained as highly crystalline powder from the solvothermal reaction of CuCl with one equivalent of $\mathbf{HL_{Na}}$ and $Et_3N$, in acetonitrile, at 130°C under 60 atm of argon. Figure S3 reports the infrared spectrum (nujol mull) of **1**, showing the disappearance of the $\nu_{NH}$ stretching, besides the expected vibrations at 1230-1180 $cm^{-1}$ ($SO_3$), 3500-3400 $cm^{-1}$ ($\nu_{OH}$) and 1655 $cm^{-1}$ (OH bending), the latter two due to lattice water. Finally, simultaneous TGA/DSC analysis was performed on **1** (0-600°C; rate: 10°C/min) (Figure S5) showing an endothermic process at 80-90°C associated to the loss of one water molecule (exper. -5.95 % *vs.* -6.46% theor.). The compound does not lose any other weight until decomposition, that starts at about 300 °C ($T_{peak}$ = 460°C).

### Structural investigation

**$\mathbf{HL_{Na}}$.** The sodium salt of 3,5-dimethyl-4-sulfonate pyrazole crystallizes in the monoclinic $P2_1/c$ space group. In its crystal structure (Figure 1), the Na ions are five-coordinated, in a (square pyramidally) distorted trigonal bipyramidal geometry by three O-atoms from three different $SO_3^-$ groups and two O-atoms of two water molecules, giving rise to the monohydrated sodium salt of formula $\mathbf{HL_{Na}}\cdot H_2O$. The structure can be described as a layered structure in which organic/inorganic/organic sandwiches (the layers) are connected through N-H···N H-bonds that propagate in a zig-zag motif along the *c* axis. This is a H-bond network frequently observed in pyrazole chemistry,[2] but a rather unique feature among the pyrazole–sulfonate structures. Indeed, the same H-bond connectivity, for pyrazole-sulfonates, has been observed only for $Sr(4\text{-}SO_3\text{-}pzH)_2$,[13] *i.e.* the strontium derivative of the not methylated pyrazole-sulfonate. The inorganic core of the sandwiches is built on a trapezoidal grid of Na-ions with Na–Na separations of 4.9286 Å, 7.1419 and 4.0222 Å interconnected by μ-(κO;$\kappa^2$-O′,O″)-bridging sulfonates and bridging water molecules, H-bonds can be found between water molecules and O-atoms of the $SO_3^-$ groups (Figure 2). Intriguingly, two hydrated sodium derivative of the not-methylated 4-pyrazole-sulfonate ligand, namely $Na(4\text{-}SO_3\text{-}pzH)(H_2O)_2$,[14] and $Na(4\text{-}SO_3\text{-}pzH)(H_2O)$,[15] have been found in the literature and both show a different crystal structure. In our system, methyl groups, other than grant a more hydrophobic nature to this ligand, may be responsible to a higher steric hindrance that prevents the pyrazoles to be organized in face-to-edge ring arrangement, as reported by Mezei et al., giving rise to the zig-zag N-H···N H-bonds network connecting the sandwich inorganic/organic layers.

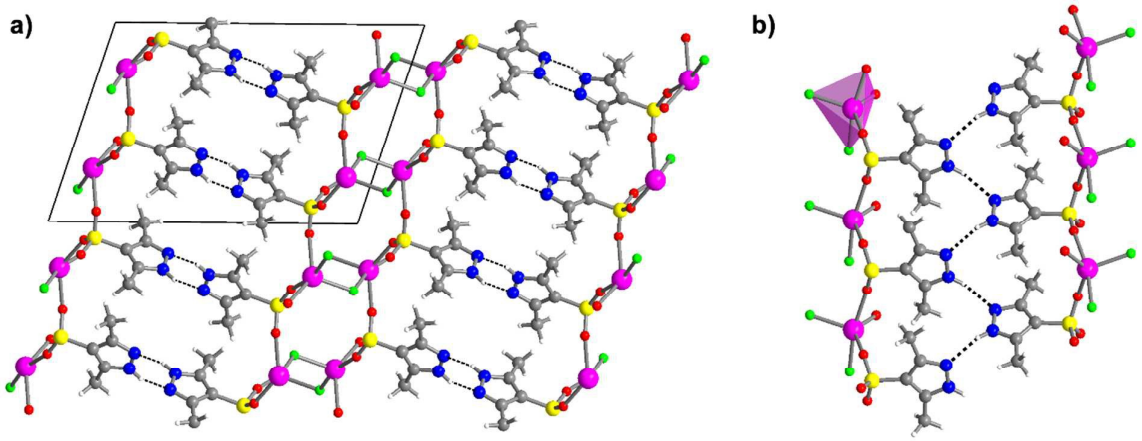


**Figure 1.** a) Crystal structure of $\mathbf{HL_{Na}}$ viewed down **b**. Horizontal axis, **a**; vertical axis, **c**. b) N-H···N hydrogen bond network running down the **b** direction. Sodium, purple; carbon, grey; nitrogen, blue; oxygen, red; water oxygen, light green; sulphur, yellow; hydrogen, white. Hydrogen bonds are drawn as fragmented black lines.

View Article Online
DOI: 10.1039/C7CE01404J

CrystEngComm

ARTICLE



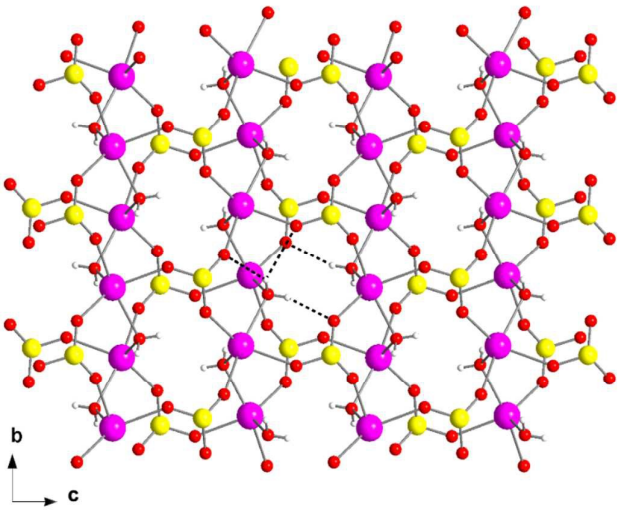


**Figure 2.** Perpendicular view to the inorganic layer of $\mathbf{HL_{Na}}$. H-bonds between water molecules and O-atoms of the $SO_3$ groups highlighted with dashed black lines. Sodium, purple; sulphur, yellow; oxygen, red; hydrogen, white.

**$\mathbf{CuL_{Na}}$.** This coordination polymer crystallizes in the *C*2/*c* space group (Figure 4). *Ab-initio* structure solution from powder diffraction data required several simulated annealing runs to find the correct structural model. This was mainly due to two issues: *i*) a very high degree of preferential orientation effects affecting this sample on the [100] direction, that have to be added as a refinable parameter in the simulated annealing runs and *ii*) the crystallographic position of the copper ions. The asymmetric unit indeed contains one water molecule, one Na ion and one ligand that all lies in general position, and two different copper ions, both in special positions and, respectively, on a C*2* axis (Wyckoff site *e,* multiplicity 4) and on an inversion center (Wyckoff site *a,* multiplicity 4). Despite these two tricky structural issues (preferential orientation effects and multiple special positions), as already successfully done in the past,[16] we were able to refine the data to a satisfactory $R_{wp}$ of 10.6 (Figure 3 and S7) and, more important, to a chemically reasonable connectivity, fully comparable with the results obtained for the $\mathbf{HL_{Na}}$ ligand. The two structures are, indeed, in some way correlated by an analogue connectivity: in $\mathbf{HL_{Na}}$ and $\mathbf{CuL_{Na}}$ hydrogens or Cu(I) atoms play the same role in connecting, with a zig-zag motif, the organic/inorganic/organic double layers.

For $\mathbf{CuL_{Na}}$, the very tight zig-zag chains of copper pyrazolates are generated by the combination of the intrinsic crystallographic position of the Cu(I) ions and their linear coordination geometry, leading to Cu-Cu intra- and inter-chain distances of 3.111 and 4.535 Å and Cu-Cu-Cu angles of 109.59 and 180° (Figure 4b). In comparison to the $\mathbf{HL_{Na}}$ linker, in the $\mathbf{CuL_{Na}}$ coordination polymer the double inorganic layer contains Na ions that are five-coordinated, in a highly distorted trigonal bipyramid (towards square pyramid), by three O-atoms of two different $SO_3^-$ groups and two water molecules (Figure 4a). Here, the trapezoidal grid, similar to that observed for $\mathbf{HL_{Na}}$, is formed by Na ions with Na-Na distances of 3.905 and 4.929 and 7.091 Å (Figure S8).

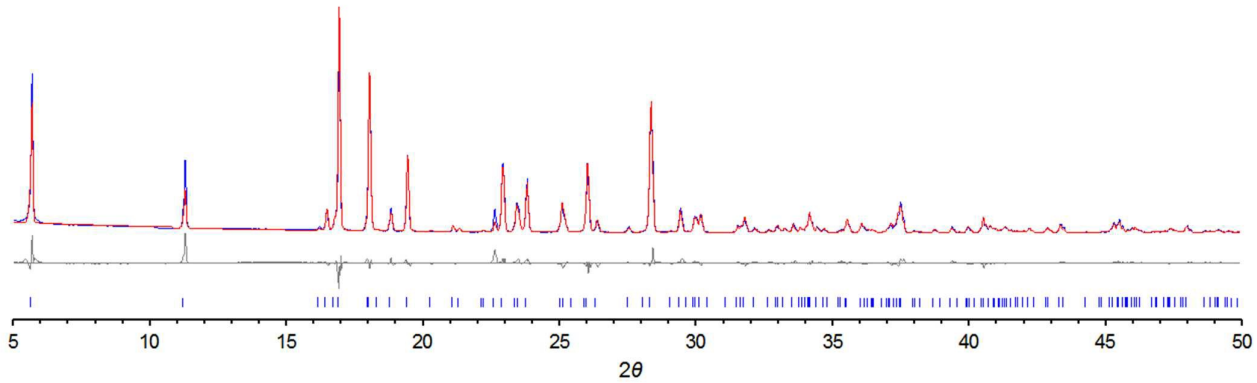


**Figure 3.** Final Rietveld refinement of $\mathbf{CuL_{Na}}$ coordination polymer in *C*2/*c* space group. $R_p$ = 0.0779; $R_{wp}$ = 0.1063 and $R_{Bragg}$ = 6.46. Blue and red lines are experimental and calculated profile, respectively. Grey line represent the difference between calculated and experimental profiles and blue thick marks represent peak positions. See Figure S7 for full profile (5-105 °) refinement.

View Article Online
DOI: 10.1039/C7CE01404J




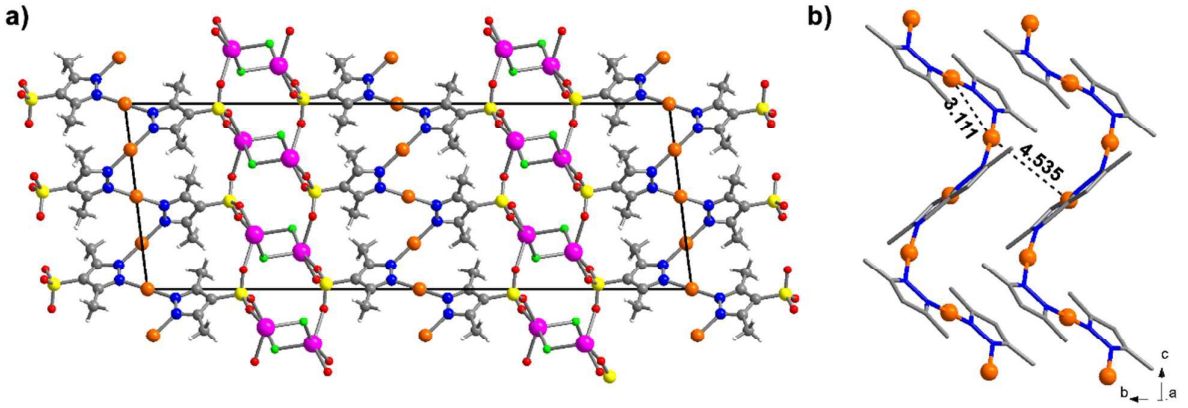


**Figure 4. a)** Crystal structure of **CuL$_{Na}$** viewed down **b**. Horizontal axis, **c**; vertical axis, **a**. **b)** Schematic depiction of inter- and intra-chain Cu···Cu separations in **CuL$_{Na}$**. Copper, orange; sodium, purple; carbon, grey; nitrogen, blue; oxygen, red; water oxygen, light green; sulphur, yellow; hydrogen, white.

With the aim of studying the dehydration process of **1** and, possibly, describing the anhydrous crystal phase of this coordination polymer, we performed an *in-situ* variable-temperature XRPD experiment. The results are reported in Figure 5. Upon heating the material, it remains stable up to 90 °C, temperature at which the peaks of the **1** phase start lowering their intensity and new peaks appear. When the dehydration process is complete (150 °C), a very low-crystallinity phase is observed and no further changes are observed up to decomposition (300 °C). Unfortunately, the very low quality of the powder pattern did not allow us to recover any structural information on the anhydrous phase of **1**. The comparison between the two powder pattern (**1** *vs* anhydrous phase) is reported in Figure 5. Once back to RT, in air, this low-crystalline anhydrous phase is not stable and absorbs water from air to give back **CuL$_{Na}$**.

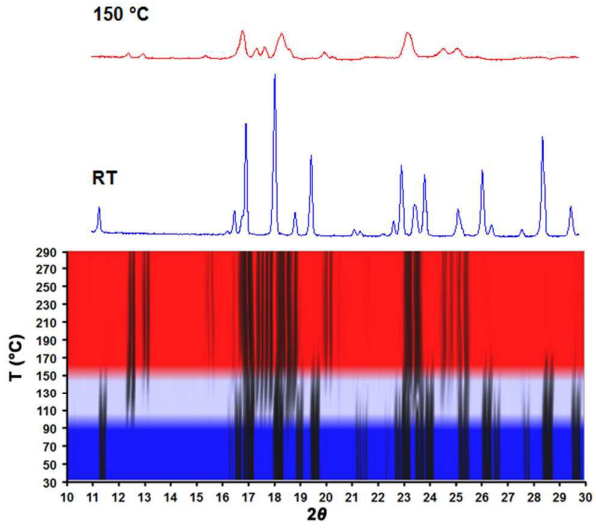


**Figure 5.** Variable-temperature X-ray powder diffraction plot (down) for **CuL$_{Na}$**. The hydrated phase is stable up to 90 °C, temperature at which new diffraction peaks appears. From 150 °C up to decomposition (300 °C) the only anhydrous phase is present and is characterized by a very low crystallinity, compared to the pristine materials (up).

**Photoluminescent behavior.** Coinage metal pyrazolate complexes often show remarkable photoluminescence performances and attractive structure-properties relations.[17] In particular, in 3,5-dimethyl pyrazolate-containing compounds, the photophysical properties can be related to both intra- and intermolecular M···M interactions, the latter originating from supramolecular stacking of cyclic [M(3,5-dmpz*)]$_3$ (3,5-Hdmpz = 3,5-dimethyl pyrazole) trimers.[5,18] Indeed, the main transition usually originates from a filled orbital with strong ligand character to a vacant molecular orbital mainly centered on the metal and showing a intramolecular M-M bonding.[5a,c] However, despite being rather weak in the electronic ground state, *inter*molecular cuprophilic interactions experience a strong enhancement in the emissive excited states, thus can also be responsible for luminescence bands in such systems.[5b]

Compound **CuL$_{Na}$** showed a remarkable luminescent behavior in the solid state. Figure 6 reports the excitation and emission spectra (a) and the lifetime decay (b) of **1** in the solid state, whereas photoluminescent data are collected in Table 1. Complex **1** is characterized by a notable yellow emission when irradiated with UV light, with $\lambda_{max}$ centered at 570 nm when $\lambda_{exc}$ = 265 nm. The emission trace is broad and unstructured, which is quite typical for coinage metals pyrazolate complexes. Worthy of note, the steady state measurements revealed an outstanding Stokes shift ($\Delta$ = 2.50 eV; 20192 cm$^{-1}$), a desirable characteristic for phosphorescent materials since could efficiently lessen self-absorption and thus would be very beneficial to light emission.[19] A good absolute quantum yield of 0.44 was also measured for **1** in the solid state. The time-resolved luminescence behavior of **CuL$_{Na}$** (Figure 6b) is described by a mono-exponential decay with $\tau$ = 21.07 (±0.03) µs, thus suggesting an excited state of triplet parentage, in accordance with what observed for other copper(I) 3,5-dimethyl pyrazolate analogues.[5]

In our compound, intra-chain Cu···Cu separations measure 3.111 Å (Figure 4b), whereas inter-chain distances are moderately long (4.535 Å). Thus, despite the expected

View Article Online
DOI: 10.1039/C7CE01404J


enhancement of these M···M interactions in the excited state as discussed above,[5b] we suppose that the phosphorescent behavior of **$CuL_{Na}$** mainly arises from *intra*molecular Cu···Cu contacts. To corroborate this, we performed DFT calculations to obtain the Natural Transition Orbitals (NTO) using the dinuclear $[Cu_2(L_{Na})_3]^-$ system as a model for the metal-ligand arrangement in the polymeric species **$CuL_{Na}$**. The choice of such a model was substantiated by the fine accordance between the solid state experimental UV trace of **$CuL_{Na}$** and the one calculated for $[Cu_2(L_{Na})_3]^-$ (Figure S12). The results of our calculations (Figure S13) show that the main transition in $[Cu_2(L_{Na})_3]^-$ (>99%) involves an electronic transfer from a filled orbital with both ligand and metal character to an empty molecular orbital predominantly centered on the adjacent copper center.

View Article Online
DOI: 10.1039/C7CE01404J

CrystEngComm

ARTICLE



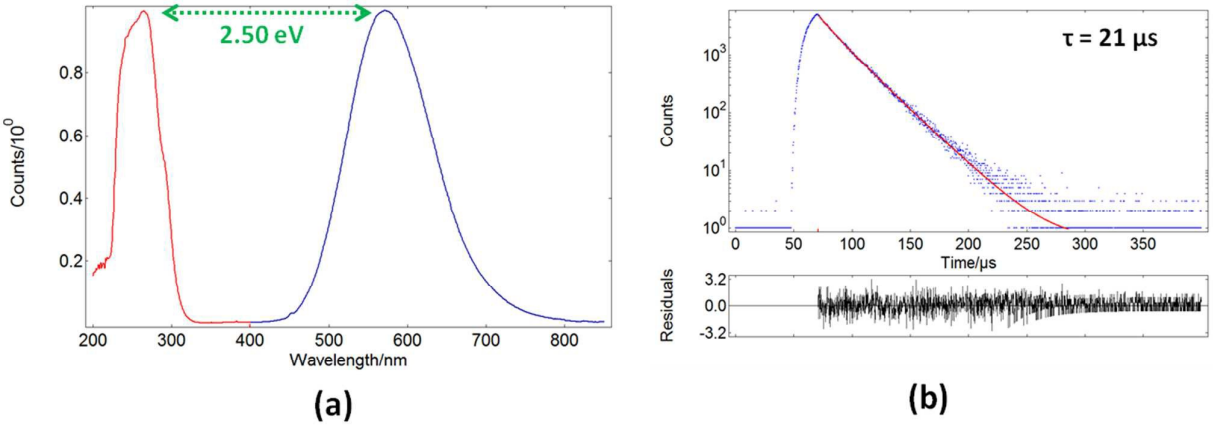


**Figure 6**. (a) Normalized excitation (red) and emission (blue) spectra of compound **1** in the solid state, with the corresponding high Stokes shift highlighted. (b) Monoexponential lifetime decay of **1** recorded in the solid state.

| | $\lambda_{exc}$ (nm)[a] | $\lambda_{max}$ (nm)[a] | $\Delta_{St}$ (eV)[b] | $\Phi_{PL}$ | τ(µs)[c] |
|---|---|---|---|---|---|
| **1** | 265 | 570 | 2.50 | 0.44 | 21.03 |

**Table 1.** Photophysical data for compound **$CuL_{Na}$** in the solid state. [a] Measurements performed on solid, crystalline sample. [b]Stokes shift. [c]Luminescent decay lifetime.

## Conclusions

In this work, we presented the synthesis of a new copper(I) coordination polymer bearing the sodium salt of 3,5-dimethyl-4-sulfonate pyrazole. The intrinsic 2D organization of **$L_{Na}$** (as deduced from the **$HL_{Na}$** structure) directs the formation of polymeric copper (I) zig-zag chains with short Cu···Cu intra- and inter-chain contacts leading to an interesting phosphorescence characterized by an intense, unstructured, yellow emission and a noteworthy Stokes shift.

## Experimental

### Materials and methods

The synthesis of the ligand was performed in water, without the need of inert atmosphere. The syntheses of the copper(I) derivative were carried out under purified nitrogen using standard Schlenk techniques. Solvents were dried and distilled according to standard procedures prior to use. Elemental analyses were obtained with a Perkin-Elmer CHN Analyzer 2400 Series II. Infrared Spectra were recorded with a Shimadzu Prestige-21 spectrophotometer (1 $cm^{-1}$ resolution). Thermogravimetric (TGA) and Differential Scanning Calorimetry (DSC) analyses were performed in a $N_2$ stream on a Netzsch STA 409 PC Luxx (heating rate 10°C/min). Solid state excitation and emission spectra were recorded using a fluorescence spectrometer (Edinburgh Instrument FS5) equipped with a 150 W continuous Xenon lamp as a light source and were corrected for the wavelength response of the instrument; lifetime measurements were performed on the same FS5 Edinburgh Instrument equipped with a LLS-270 Ocean Optics LED Light Source (wavelength 270 nm; FWHM 12 nm; power 15 µW) as the pulsed source. as the pulsed source. Analysis of the lifetime decay curve was performed using Fluoracle® Software package (Ver. 1.9.1) which runs the FS5 Edinburgh Instrument. Absolute fluorescence quantum yields were determined on a Photon Technologies International QuantaMaster QM-40 spectrometer (equipped with Xe arc lamp, 70 W) using a PhotoMed GmbH K-Sphere Integrating Sphere (3.2 inch. diameter). $Cu(CH_3CN)_4BF_4$[20] and CuCl[21] were prepared as reported in the literature. All other chemicals were of reagent grade quality, were purchased commercially (Aldrich, TCI Chemicals) and used as received.

**Synthesis of 3,5-dimethyl-1*H*-pyrazole-4-sulfonate barium salt ($HL_{Ba}$).**[12] In a 50 mL flask, 3,5-dimethyl-1*H*-pyrazole (3 g, 31.20 mmol) was dissolved in 10 mL of fuming sulphuric acid (30% free $SO_3$ basis), while keeping the reaction temperature at 0°C. Once the dissolution was completed and the fuming has ceased, the solution was heated at 60°C for 6 h. Then, after cooling to room temperature, the solution was poured into a 500 mL flask, diluted with water (300 mL) and cautiously neutralized by addition of small portions of $BaCO_3$ (up to ca. 60 g) until no gas evolution was noticed. The solid formed ($BaSO_4$) was removed by filtration, and the filtrate aqueous solution was concentrated to dryness by rotary evaporation. The white solid residue was collected with acetone, filtered and dried in vacuo. Yield 7.10 g (90%). Elemental analysis (%) calcd. for $C_{10}H_{16}BaN_4O_7S_2$: C 23.75, H 3.19, N 11.08. Found C 23.80, H 3.01, N 10.94 %.

**Synthesis of 3,5-dimethyl-1*H*-pyrazole-4-sulfonate sodium salt ($HL_{Na}$).** In a 50 mL flask, a solution of $Na_2SO_4$ (0.281 g, 1.978 mmol) in water (5 mL) was slowly added to a solution of **$HL_{Ba}$** (1.0 g, 1.977 mmol) in 10 mL of water, causing the immediate precipitation of $BaSO_4$. The solid was removed by filtration and rinsed with water (10 mL). The combined aqueous filtrate was concentrated to dryness by rotary evaporation, then the residue was boiled in hot ethanol for 1 h, filtered when hot (to remove any residual $Na_2SO_4$)

View Article Online
DOI: 10.1039/C7CE01404J




and the solution was concentrated to dryness, giving a white solid. Yield 0.83 g (97%). Elemental analysis (%) calcd. for $C_5H_9N_2NaO_4S$: C 27.78, H 4.20, N 12.96. Found C 27.75, H 4.00, N 12.83 %. IR ($cm^{-1}$; see Figures S1-S2): 3518, 3421 (OH); 3170, 3110 (NH); 2975, 2869 ($CH_3$); 1644 (OH), 1574 (C=N); 1225, 1185 ($SO_3$).

**Synthesis of $CuL_{Na}$ (1).** a) In a schlenk, $HL_{Na}$ (0.140 g, 0.648 mmol) and $Cu(CH_3CN)_4BF_4$ (0.200 g, 0.636 mmol) were suspended in $CH_3CN$ (20 mL), then $Et_3N$ (0.5 mL, 3.594 mmol) was added. The white suspension was gently refluxed for 6 h. Then the suspension was filtered under inert atmosphere when hot, and the white solid washed with $CH_3CN$, and then dried under a flux of nitrogen. Yield 0.140 g (79%). Elemental analysis (%) calcd. for $C_5H_8CuN_2NaO_4S$: C 21.55, H 2.89, N 10.05. Found C 21.58, H 2.80, N 10.19 %. IR ($cm^{-1}$; see Figures S3-S4): 3506, 3404 (OH); 2969, 2921 ($CH_3$); 1655 (OH), 1574 (C=N); 1231, 1180 ($SO_3$).

b) In a steel autoclave previously purged with nitrogen, 25 mL of $CH_3CN$ were thoroughly deoxygenated, then CuCl (0.063 g, 0.636 mmol) and $HL_{Na}$ (0.140 g, 0.648 mmol) were added and the suspension further deoxygenated for other 30 minutes. Then $Et_3N$ was added (0.5 mL, 3.594 mmol) and the autoclave was charged with 60 atm of argon. The system was heated at 130°C for 3 h; after slowly cooling to room temperature, the autoclave was vented, the suspension was filtered and the white, crystalline solid was stored under nitrogen. Yield 0.158 g (89%). Elemental analysis (%) calcd. for $C_5H_8CuN_2NaO_4S$: C 21.55, H 2.89, N 10.05. Found C 21.50, H 2.78, N 9.98 %.

**Single crystal XRD structure determination of $HL_{Na}$.**

The crystal was mounted on a Bruker AXS APEXII CCD area-detector diffractometer, at room temperature for the unit cell determination and data collection. Graphite-monochromatized Mo Kα (λ = 0.710 73 Å) radiation was used with the generator working at 50 kV and 30 mA. Orientation matrixes were initially obtained from least-squares refinement on ca. 300 reflections measured in three different ω regions, in the range 0° < θ < 23°; cell parameters were optimized on the position, determined after integration, of ca. 8000 reflections. The intensity data were retrieved in the full sphere, within the θ limits reported in the crystal data section, from 1080 frames collected with a sample–detector distance fixed at 5.0 cm (50 s $frame^{-1}$ ; ω scan method, Δω = 0.5°). An empirical absorption correction was applied (SADABS)[22]. Crystal structure was solved by direct methods using SHELXT2017 and refined with SHELXL-2017/1,[23,24] within the Wingx suite of programs.[25] Hydrogen atoms were riding on their carbon atoms. Anisotropic temperature factors were assigned to non-hydrogen atoms. Crystal data collection and refinement parameters are listed below and in the cif files. A view of the molecule with the full numbering scheme is given in Figure S11. Selected distances of bond lengths (Å) are given in Table S1, while atomic coordinates and displacement parameters are listed in the cif file.

***Ab-initio* Crystal Sructure Detrmination of $CuL_{Na}$ from Powder Diffraction Data.**

Gently ground powders of $CuL_{Na}$ were deposited in the, 2 mm deep, hollow of a zero background plate (a properly misoriented quartz monocrystal). Diffraction experiments were performed using Cu-$K_\alpha$ radiation (λ = 1.5418 Å) on a vertical-scan Bruker AXS D8 Advance diffractometer in θ:θ mode, equipped with a Goebel Mirror and a Bruker Lynxeye linear Position Sensitive Detector (PSD), with the following optics: primary and secondary Soller slits, 2.3° and 2.5°, respectively; divergence slit, 0.1°; receiving slit, 2.82°. Generator setting: 40 kV, 40 mA. The nominal resolution for the present set-up is 0.08° 2θ (FWHM of the $\alpha_1$ component) for the $LaB_6$ peak at about 21.3° (2θ). The accurate diffraction patterns at RT $CuL_{Na}$ compound was acquired in the 5–105° 2θ range, with Δ2θ = 0.02° and exposure time 5 s/step. A standard peak search below 30° was followed by indexing through the singular value decomposition method,[26] implemented in TOPAS-R,[27] which led to a monoclinic *C* cell of approximate dimensions: a = 31.62 Å , b = 5.55 Å, c = 10.82 Å, β = 96.98 and V = 1884 $Å^3$ (GoF(20) = 49.65). Systematic absences and volume considerations led to individuate *C*2/c as the most probable space group, with Z = 8. Prior to structure solution, a Le Bail refinement was carried out (a = 31.6264 Å , b = 5.5506 Å, c = 10.8285 Å and β = 96.969; $R_{wp}$ 8.692) in order to determine the background, cell and profile parameters to be used in the subsequent simulated annealing runs. A preliminary structural model was determined *ab initio* by the simulated annealing approach implemented in TOPAS-R. A rigid body was used to describe the $L_{Na}$ ligand.[28] A torsion angle around the C1-S1 bond, connecting the pyrazolate to the $SO_3^-$ fragments, was let to refine. The peak shapes were described with the fundamental parameters approach[29] and with the aid of spherical harmonics. The background was modelled by a Chebyshev polynomial function. The thermal effect was simulated by using a single isotropic parameter for the metal ion, augmented by 2.0 $Å^2$ for lighter atoms. To reach the final structural model, several simulated annealing runs were necessary. A preferential orientation phenomena on the [100] crystallographic direction was let to refine during simulated annealing runs. The position of the Cu ions was determined *i*) assuming a similar connectivity of the one observed for the $HL_{Na}$ ligand, in which pyrazole N-H hydrogen atoms where possibly been replaced by Cu(I) ions and *ii*) by looking closely at the symmetry operation of the *C*2/*c* space group. The final Rietveld refinement plot is supplied in Figure 3. Fractional atomic coordinates are provided with the Supporting Information as CIF file.

*Crystal data for $HL_{Na}$ compound:* $C_5H_9N_2NaO_4S$, *fw* = 216.19 $gmol^{-1}$, monoclinic $P2_1/c$ (No. 14), a =15.883(7), b = 5.585(4) and c = 10.779(10) Å, β = 108.170(10); V = 908.5(11) $Å^3$ , Z = 4, Mo-$K_\alpha$ λ = 0.71073 Å, T (K) 293(2); $\rho_{calc}$ =1.581 g $cm^{-3}$, μ(Mo-$K_\alpha$) = 0.39 $mm^{-1}$; θ range 2.699 - 27.054 °; data (unique), 7973 (1993); restraints, 0; parameters, 120; Goodness-of-Fit on $F^2$, 1.111; $R_1$ and $wR_2$ (I>2σ(I)), 0.0514 and 0.0952; $R_1$ and $wR_2$ (all data), 0.0785 and 0.1012; Largest Diff. Peak and Hole (e $Å^{-3}$), 0.637 and -0.428.

*Crystal data for $CuL_{Na}$ compound:* $CuC_5H_8N_2NaO_4S$, fw = 278.73 $gmol^{-1}$, monoclinic *C*2/*c* (No. 15), a = 31.6114(5), b = 5.5479(14) and c = 10.8229(30) Å, β = 96.974(20); V = 1884.046(8) $Å^3$ , Z = 8, Cu-$K_\alpha$ λ = 1.5418 Å, T(K), 293(2); $\rho_{calc}$ = 1.9511 g $cm^{-3}$ , μ(Cu-$K_\alpha$) = 57.823 $cm^{-1}$. $R_p$ and $R_{wp}$ 0.0779 and 0.1063 respectively, for 5001 data collected in the 5–105 ° 2θ range. $R_{Bragg}$ = 0.0646.

Crystallographic data in CIF format have been deposited at the Cambridge Crystallographic Data Centre as supplementary publication No. 1565784-1565785 Copies of the data can be obtained free of charge on application to the Director, CCDC, 12 Union Road, Cambridge, CB2 1EZ, UK (Fax: +44-1223-335033; e-mail: deposit@ccdc.cam.ac.uks or http://www.ccdc.cam.ac.uk).

**Thermodiffractometry**

Variable-temperature X-ray powder diffraction (VT-XRPD) experiments were performed on $CuL_{Na}$. The experiment was carried out in air and in nitrogen atmosphere with comparable results by coupling a custom-made sample heater, assembled by Officina Elettrotecnica di Tenno, Ponte Arche, Italy, to the instrumental set-up described above. A powdered microcrystalline sample was ground in an agate mortar and was deposited in the hollow of on a quartz zero-background plate framed by an aluminium skeleton. The data were acquired within a sensible, low-angle 2θ range, heating the samples in situ in the temperature range 30-300 °C, with steps of 20 °C. The VT diffractograms are depicted in Figure 3 and Figure S9. *When comparing TGA and VTXRPD results, the reader must be aware that the thermocouple of the VT-XRPD set-up is not in direct contact with the sample, this determining a slight difference in the temperature at which the same event is detected by the two techniques. The TGA temperatures have to be considered as more reliable.*

## Conflicts of interest

There are no conflicts to declare.

View Article Online
DOI: 10.1039/C7CE01404J




## Acknowledgements

S.B. and G.A.A. thanks Ministero dell'Istruzione, dell'Università e della Ricerca (MIUR), the University of Insubria (grant CSR-12) for financial support. S.B. acknowledges Fondazione Banca del Monte di Lombardia (FBML) for generous funding through the Research Project "*Transition-metals based coordination compounds for light emitting device applications*". V.C. appreciates partial funding from the Università degli Studi di Milano (Unimi) through the Development Plan of Athenaeum grant – ACTION B (PSR2015-1716FDEMA_07).

## Notes and references

1 A. A. Mohamed, *Coord. Chem. Rev.* 2010, **254**, 1918-1947.
2 T. Jozak, Y. Sun, Y. Schmitt, S. Lebedkin, M. Kappes, M. Gerhards and W. R. Thiel, *Chem. Eur. J.* 2011, **17**, 3384-3389.
3 N. Masciocchi, M. Moret, P. Cairati, A. Sironi, G.A. Ardizzoia and G. La Monica, *J. Am. Chem. Soc.* 1994, **116**, 7668-7676.
4 C.-Y. Zhang, J.-B. Feng, Q. Gao and Y.-B. Xie, Acta Crystallogr. 2008, **E64**, m352.
5 (a) Y. Morishima, D. J. Young and K. Fujisawa, *Dalton Trans.* 2014, **43**, 15915-15928. (b) H. V. Rasika Dias, H. V. K. Diyabalanage, M. G. Eldabaja, O. Elbjeirami, M. A. Rawashdeh-Omary and M. A. Omary, *J. Am. Chem. Soc*. 2005, **127**, 7489-7501. (c) M. A. Omary, M. A. Rawashdeh-Omary, M. W. A. Gonser, O. Elbjeirami, T. Grimes, T. R. Cundari, H. V. K. Diyabalanage, C. S. P. Gamage and H. V. Rasika Dias, *Inorg. Chem*. 2005, **44**, 8200-8210.
6 (a) G. A. Ardizzoia, S. Cenini, G. La Monica, N. Masciocchi and M. Moret, *Inorg. Chem.* 1994, **33**, 1458-1463. (b) A. Maspero, S. Brenna, S. Galli, A. Penoni, *J. Organomet. Chem.* 2003, **672**, 123-129.
7 F. Gong, Q. Wang, J. Chen, Z. Yang, M. Liu, S. Li, G. Yang, L. Bai, J. Liu and Y. Dong, *Inorg. Chem.* 2010, **49**, 1658-1666.
8 See e.g. (a) G. A. Ardizzoia, S. Brenna, S. Durini and B. Therrien, *Organometallics* 2012, **31**, 5427-5437; (b) G. A. Ardizzoia, S. Brenna and B. Therrien, *Dalton Trans*. 2012, **41**, 783-790; (c) D. Tzimopoulos, S. Brenna, A. Czapik, M. Gdaniec, A. Ardizzoia and P. D. Akrivos, Inorg. Chim. Acta 2012, **383**, 105-111. (d) G. A. Ardizzoia, S. Brenna and B. Therrien, *Eur. J. Inorg. Chem*. 2010, 3365-3371; (e) G. A. Ardizzoia, S. Brenna, F. Castelli, S. Galli and N. Masciocchi, *Inorg. Chim. Acta* 2010, **363**, 324-329; (f) G. C. Shearer, V. Colombo, S. Chavan, E. Albanese, B. Civalleri, A. Maspero, S. Bordiga *Dalton Trans*. 2013, **42,** 6450-6458. (g) V. Colombo, C. Montoro, A. Maspero, G. Palmisano, N. Masciocchi, S. Galli, E. Barea, J. A. R. Navarro *J. Am. Chem. Soc.* 2012, **134**, 12830-12843.
9 (a) G. A. Ardizzoia, S. Brenna, S. Durini, I. Trentin and B. Therrien, *Dalton Trans*. 2013, **42**, 12265-12273. (b) V. Colombo, S. Galli, H.J. Choi, G.D. Han, A. Maspero, G. Palmisano, N. Masciocchi, J.R. Long *Chemical Science* **2**, 1311-1319.
10 (a) G. A. Ardizzoia, S. Brenna, F. Castelli, S. Galli, C. Marelli and A. Maspero, *J. Organomet. Chem*. 2008, **693**, 1870-1876. (b) V. Colombo, A. Maspero, L. Nardo, A. Aprea, F. Linares, A. Cimino, S. Galli *Polyhedron* 2015, **92**, 130–136.
11 (a) G. A. Ardizzoia, S. Brenna, S. Durini, B. Therrien and M. Veronelli, *Eur. J. Inorg. Chem*. 2014, 4310-4319. (b) G. A. Ardizzoia, S. Brenna, S. Durini and B. Therrien, *Polyhedron* 2015, **90**, 214-220. (c) S. Durini, G. A. Ardizzoia, B. Therrien and S. Brenna, *New. J. Chem.* 2017, **41**, 3006-3014.
12 G. T. Morgan, I. Ackerman, *J. Chem. Soc.* 1923, 1308-1318.
13 I. R. Fernando, N. Daskalakis, K. D. Demadis, G. Mezei, *New J. Chem.* 2010, **34**, 221–235.
14 G. Mezei, R. G. Raptis, *New J. Chem.* 2003, **27**, 1399–1407.
15 I. R. Fernando, S. Jianrattanasawat, N. Daskalakis, K. D. Demadis, G. Mezei *CrystEngComm* 2012, **14**, 908–919.
16 See e.g. (a) B. Tasso, G. Pirisino, F. Novelli, D. Garzon, R. Fruttero, F. Sparatore, V. Colombo, A. Sironi *Tetrahedron* 2014, **70**, 8056–8061. (b) M. R. Chierotti, R. Gobetto, C. Nervi, A. Bacchi, P. Pelagatti, V. Colombo, A. Sironi, A. *Inorg. Chem.* 2014, **53**, 139–146, (c) V. Colombo, A. Cimino, A. Maspero, G. Palmisano, A. Sironi *Solid State Sciences* 2017, **71**, 22-28.
17 (a) M. A. Omary, O. Elbjeirami, C. S. Palehepitiya Gamage, K. M. Sherman and H. V. R. Dias, *Inorg. Chem.* 2009, **48**, 1784-1786. (b) L. Hou, W-J. Shi, Y-Y. Wang, H-H. Wang, L. Cui, P-X. Chen, Q-Z. Shi, *Inorg. Chem.* 2011, **50**, 261-270. (c) L-Y. Du, W-J. Shi, L. Hou, Y-Y. Wang, Q-Z. Shi, Z. Zhu, *Inorg. Chem.* 2013, **52**, 14018-14027.
18 W.-X. Ni, M. Li, J. Zheng, S.-Z. Zhan,; Y.-M. Qiu, S. W. Ng, D. Li, *Angew. Chem. Int. Ed.* 2013, **52**, 13472-13476.
19 X. Li, D. Zhang, G. Lu, G. Xiao, H. Chi, Y. Dong, Z. Zhang, Z. Hu, *J. Photochem. Photobiol. A: Chemistry* 2012, **241**, 1– 7.
20 G. J. Kubas, Inorg. Synth. 1979, **19**, 90-92.
21 R. N. Keller, H. D. Wycoff, *Inorganic. Syntheses* Vol. II (1946) pp. 1-4, Ed. by W. C. Fernelius, McGraw-Hill Book Co., Inch. USA.
22 Sheldrick, G. M. *SADABS*, Program for Absorption Correction; University of Göttingen, Göttingen, Germany, 1996.
23 Sheldrick, G. M. *Acta Crystallogr.* 2008, **A64**, 112.
24 G. M. Sheldrick, SHELXL, University of Göttingen, Germany, 2014.
25 L. J. Farrugia, *J. Appl. Cryst.* 2012, **45**, 849-854.
26 A. Coelho, *J. Appl. Crystallogr.*, 2003, **36**, 86.
27 TOPAS Version 3.0, Bruker AXS, Karlsruhe, Germany 2005.
28 The dm-Pz-SO3 moiety was modelled as a rigid body by means of the z-matrix syntax, adopting idealized bond angles and distances: C–C, C–N of the penta-atomic rings = 1.36 Å; penta-atomic rings internal bond angles = 108°; penta-atomic rings external bond angles = 126°; S-O distances = 1.45; C-S distance = 1.744.
29 R.W. Cheary, A. Coelho, *J. Appl. Cryst.*, 1992, **25**, 109.



 

View Article Online
DOI: 10.1039/C7CE01404J

graphical abstract

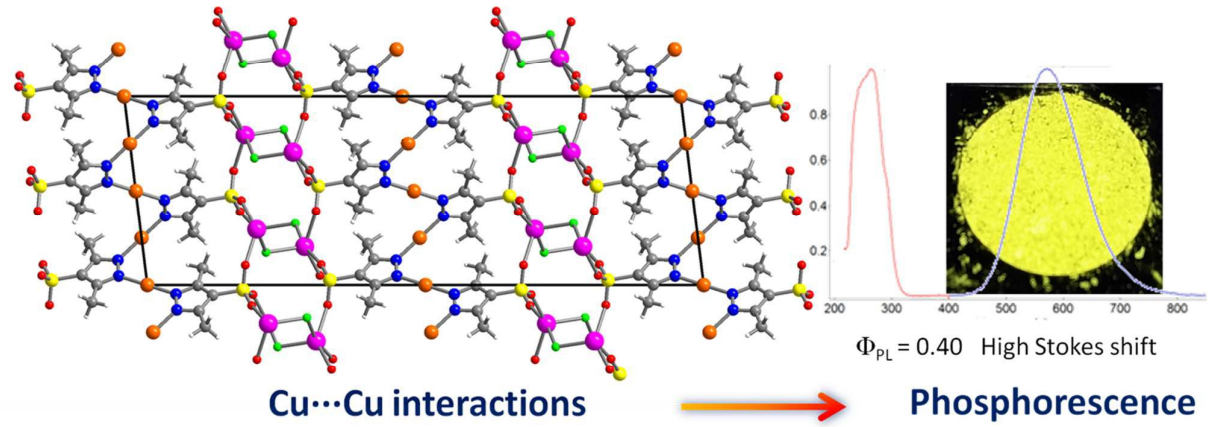


A phosphorescent copper(I) coordination polymer has been synthesized and characterized via *ab initio* PXRD.